# Rapid Iodine Oxoacids Nucleation Enhanced by Dimethylamine in Broad Marine Regions

Haotian Zu<sup>1</sup>, Biwu Chu<sup>2</sup>, Yiqun Lu<sup>3</sup>, Ling Liu<sup>1\*</sup>, Xiuhui Zhang<sup>1\*</sup>

<sup>1</sup>Key Laboratory of Cluster Science, Ministry of Education of China, School of Chemistry and Chemical Engineering, Beijing Institute of Technology, Beijing 100081, China

<sup>2</sup>State Key Joint Laboratory of Environment Simulation and Pollution Control, Research Center for Eco-Environmental Sciences, Chinese Academy of Sciences, Beijing 100085, China

<sup>3</sup>State Environmental Protection Key Laboratory of Formation and Prevention of Urban Air Pollution Complex, Shanghai Academy of Environmental Sciences, Shanghai 200233, China

10 Correspondence to: Ling Liu (lingliu@bit.edu.cn) and Xiuhui Zhang (zhangxiuhui@bit.edu.cn)

**Abstract.** Recent experiments revealed a vital nucleation process of iodic acid (HIO<sub>3</sub>) and iodous acid (HIO<sub>2</sub>) under the marine boundary layer conditions. However, HIO<sub>3</sub>-HIO<sub>2</sub> nucleation may not effectively drive the observed rapid new particle formation (NPF) in certain coastal regions influenced by urban air masses. Dimethylamine (DMA) is a promising basic precursor to enhance nucleation considering its strong ability to stabilize acidic clusters and the wide distribution in marine atmosphere, while its role in HIO<sub>3</sub>-HIO<sub>2</sub> nucleation remains unrevealed. Hence, a method combining quantum chemical calculations and Atmospheric Cluster Dynamics Code (ACDC) simulations was utilized to study the HIO<sub>3</sub>-HIO<sub>2</sub>-DMA nucleation process. We found that DMA can preferentially accept the proton from HIO<sub>3</sub> as a basic precursor in the most stable configurations of HIO<sub>3</sub>-HIO<sub>2</sub>-DMA clusters. Kinetically, the participation of DMA in the cluster formation pathways of iodine oxoacids system could be significant at 10<sup>-1</sup> - 1 pptv level of [DMA]. Furthermore, DMA can enhance the cluster formation rates of the HIO<sub>3</sub>-HIO<sub>2</sub>-BMA mechanism near DMA sources for more than 10<sup>3</sup>-fold. Compared to the classical nucleation mechanism, the HIO<sub>3</sub>-HIO<sub>2</sub>-DMA mechanism exhibits strong nucleation ability, worthy of consideration as a promising mechanism in marine and polar regions rich in amine sources. The newly proposed HIO<sub>3</sub>-HIO<sub>2</sub>-DMA ternary mechanism might provide an explanation for some missing fluxes of atmospheric iodine particles.

#### 1 Introduction

5

15

20

25

30

35

Atmospheric aerosols, the intricate suspension formed by fine particles in the atmosphere, exert far-reaching influences on global climate (Haywood and Boucher, 2000; Murphy and Ravishankara, 2018; Lee et al., 2019), radiation balance (Haywood and Boucher, 2000), and human health (Pope and Dockery, 2006; Gong et al., 2014). A significant source of atmospheric aerosols on the world-wide scale is the new particle formation (NPF), encompassing nucleation and subsequent growth (Zhang, 2010). The nucleation is identified as the key process of NPF events. Therefore, understanding the nucleation mechanism is vital for comprehending the behavior of aerosols (Zhang et al., 2012; Kalivitis et al., 2015).

Sulfuric acid (H<sub>2</sub>SO<sub>4</sub>) is considered a crucial precursor for the nucleation in continental regions. However, under actual atmospheric conditions, the H<sub>2</sub>SO<sub>4</sub>-Water (W) binary nucleation is far from sufficient to explain the observed strong NPF events (Elm, 2021a). Therefore, additional components are essential for nucleation. Specifically, abundant atmospheric bases, such as ammonia (A) and alkylamines [methylamine (MA), dimethylamine (DMA), trimethylamine (TMA), and ethylenediamine (EDA)] (Weber et al., 1996; Kurtén et al., 2008; Kirkby et al., 2011; Elm et al., 2017; Xie and Elm, 2021), are recognized as important stabilizers for H<sub>2</sub>SO<sub>4</sub>-driven nucleation. Computational work by Kurtén et al. (Kurtén et al., 2008) and experimental studies by Almeida et al. (Almeida et al., 2013) indicated that, despite the lower atmospheric concentration of DMA (few pptv.), the promoting effect of DMA on the H<sub>2</sub>SO<sub>4</sub>-driven nucleation rate is several orders of magnitude higher than that of A. Moreover, nitric acid (NA) is also a potential precursor in the nucleation process (Knattrup

and Elm, 2022). Liu et al. (Liu et al., 2018; Liu et al., 2021a) showed the significant promoting effect of NA on the classical H<sub>2</sub>SO<sub>4</sub>-A and H<sub>2</sub>SO<sub>4</sub>-DMA nucleation mechanisms by theoretical methods. Additionally, Wang et al. (Wang et al., 2020) studied the nucleation process of mixed vapor of NA and A under atmospheric conditions in the CLOUD chamber at the European Organization for Nuclear Research, and subsequently considered the promoting effect of H<sub>2</sub>SO<sub>4</sub> on NA-A system (Wang et al., 2022).

45

50

55

60

65

70

75

80

85

Given the vast expanses of the ocean, marine aerosols play an indispensable role in the global aerosol system (O'Dowd and de Leeuw, 2007). Over the oceans, H<sub>2</sub>SO<sub>4</sub> and methanesulfonic acid (MSA), the oxidation products of dimethylsulfide (DMS), is considered as important nucleation precursors over the oceans (Elm, 2021b). Theoretical calculations (Chen et al., 2020a; Chen et al., 2020b; Shen et al., 2020) have indicated that basic precursors such as A, MA, and DMA can promote MSA-based nucleation processes. However, a recent study on aerosol acidity showed that global models substantially overestimate the concentrations of A, especially in polar regions (Nault et al., 2021). This may slightly weaken the influence of H<sub>2</sub>SO<sub>4</sub>-based and MSA-based nucleation in marine atmosphere (He et al., 2023). In recent years, the iodine species, originate from biological emissions of marine macroalgae (O'Dowd et al., 2002c; O'Dowd et al., 2002b; Zhang et al., 2012; O'Dowd et al., 2002a), are also thought to be important precursors of the frequent NPF events in marine and polar regions (Hoffmann, O'Dowd and Seinfeld, 2001; Ehn et al., 2010; McFiggans et al., 2010; Mahajan et al., 2011; Baccarini et al., 2020). Several studies have consistently highlighted the pivotal role of iodic acid (HIO3) in marine nucleation processes (Yu et al., 2019; Baccarini et al., 2020; Rong et al., 2020; Xia et al., 2020; He et al., 2021; Sipilä et al., 2016). Molecular-level observations conducted at the Mace Head coastal station in Ireland have provided evidence that the nucleation process is predominantly driven by HIO<sub>3</sub> with high concentration of 10<sup>8</sup> molecules cm<sup>-3</sup> (Sipilä et al., 2016). Iodous acid (HIO<sub>2</sub>) was also detected in both gas (up to 2×106 molecules cm<sup>-3</sup>) and particle phases during the NPF events together with the HIO<sub>3</sub> (Yu et al., 2019; Sipilä et al., 2016). Recently, HIO<sub>2</sub> has been confirmed to play an important role in stabilizing the neutral HIO<sub>3</sub> clusters in the Cosmics Leaving OUtdoor Droplets (CLOUD) chamber in European Organization for Nuclear Research (CERN) (He et al., 2021). This was found to be concerned with the base-like behavior of HIO<sub>2</sub> in HIO<sub>3</sub>-HIO<sub>2</sub> clusters by subsequent theoretical studies (Zhang et al., 2022a; Liu et al., 2023). In short, the iodine oxoacids (HIO<sub>x</sub>, x = 2, 3) can drive rapid particle formation, and they may play an important role in marine and polar NPF process. However, in certain coastal areas influenced by urban air masses, such as the Zhejiang region, former studies indicated that iodine species could drive nucleation processes, while the HIO3-HIO2 nucleation mechanism may not sufficiently explain the field observation results (Yu et al., 2019; Ma et al., 2023; Zu et al., 2024; Xia et al., 2020), which indicates that other nucleation precursors may be involved.

In addition to iodine species, dimethylamine (DMA) is also a common nucleation precursor in the oceanic atmosphere (Facchini et al., 2008). DMA can originate from plankton and bacteria in seawater (Müller et al., 2009; Hu et al., 2015; Chen et al., 2021). Ice-influenced ocean may also be important sources of DMA (Dall'Osto et al., 2017; Dall'Osto et al., 2019). Moreover, the industrial activities also generate a large amount of DMA-containing pollutants (Corral et al., 2022). Hence, DMA is widely distributed and abundant under the different oceanic atmospheric conditions, displaying a spatial distribution remarkably akin to that of iodine species in mid-latitudes coastal and high-latitudes polar regions (Vanneste, Duce and Lee, 1987; Gronberg, Lovkvist and Jonsson, 1992; Gibb, Mantoura and Liss, 1999; Quéléver et al., 2022). DMA has strong base-stabilization effect on the H<sub>2</sub>SO<sub>4</sub>-based nucleation process (Almeida et al., 2013; Yao et al., 2018) since it possesses relatively strong basicity. Therefore, DMA may participate in and facilitate the iodine oxoacids nucleation through similar acid-base interactions with H<sub>2</sub>SO<sub>4</sub>-DMA system. However, previous studies have not adequately explored the influence of DMA on the iodine oxoacids (HIO<sub>3</sub> and HIO<sub>2</sub>) nucleation in marine regions, and the ternary nucleation mechanism of HIO<sub>3</sub>-HIO<sub>2</sub>-DMA remains to be disclosed.

In the present study, the nucleation mechanism of HIO<sub>3</sub>-HIO<sub>2</sub> enhanced by DMA under atmospheric conditions of different marine regions (mid-latitudes coastal and high-latitudes polar regions) were studied by a method combining quantum chemical calculation and Atmospheric Cluster Dynamics Code (ACDC) model. The simulated system contains (HIO<sub>3</sub>)<sub>x</sub>·(HIO<sub>2</sub>)<sub>y</sub>·(DMA)<sub>z</sub> ( $1 \le x + y + z \le 6$ ;  $x + y \ge z$ ) clusters. The largest clusters with a mobility diameter (Almeida et al., 2013) up to 1.3 nm in the size range of nucleation clusters (Zhang et al., 2012) are stable enough to resist evaporation at the studied temperature, and clusters with more DMA molecules (x + y < z) are usually unstable. This study aims to reveal the

potential role of DMA in the HIO<sub>3</sub>-HIO<sub>2</sub> nucleation and help to better understand the intensive NPF events in broad marine regions.

## 2 Method

90

95

100

105

110

115

120

125

130

## 2.1 Quantum chemical calculations

The HIO<sub>3</sub>-HIO<sub>2</sub>-DMA system is composed of ternary clusters (HIO<sub>3</sub>-HIO<sub>2</sub>-DMA), binary clusters (HIO<sub>3</sub>-HIO<sub>2</sub>, HIO<sub>3</sub>-DMA,  $HIO_2$ -DMA) and the pure  $HIO_x$  (x = 2, 3) clusters. The most stable configuration of  $HIO_3$ - $HIO_2$ -DMA ternary clusters and HIO2-DMA binary clusters were proposed in this study for the first time. Additionally, the structures of HIO3- $HIO_2/DMA$  clusters and pure- $HIO_x$  (x = 2, 3) clusters presented in this work were adopted from the stable configurations with the lowest Gibbs free energy of formation in previous studies (Rong et al., 2020; Ning et al., 2022; Zhang et al., 2022b; Liu et al., 2023) at the same level of theory. A multi-step searching progress that can systematically screen the structures of clusters was adopted in this research. Firstly, the ABCluster program (Zhang and Dolg, 2015) was performed to generate up to 120000 initial isomer structures using the artificial bee algorithm (details in Section S1 of Supporting Information). The universal force field (UFF) (Rappé et al., 1992) was chosen to select up to 1000 structures with lower energies from the initial isomer structures. Due to the inability of the UFF force field to effectively handle bond breaking issues, we also utilized ion monomers for sampling during the configuration search of ternary clusters (Kubecka et al., 2019). From the most stable configuration of binary HIO2-DMA clusters (Figure S3), it showed that the proton transfer from HIO2 to DMA is forbidden in all cluster except for (HIO<sub>2</sub>)<sub>1</sub>(DMA)<sub>1</sub>, indicating that this process is difficult to occur spontaneously. Hence, we only considered the ion monomers where HIO<sub>3</sub> donates protons or HIO<sub>2</sub>/DMA accept proton. Secondly, 1000 structures for each cluster were pre-optimized by the PM7 semi-empirical method (Stewart, 2013) with Mopac 2016 program (Stewart, 2016) to choose 100 structures with relatively low energies. Then 100 structures were optimized at the ωB97X-D/6-31+G\* (for H, C, N and O atoms) + Lanl2DZ (for I atom) level of theory (Yang, Weaver and Merz, 2009; Elm, 2013) to find out 10 relatively stable structures of all. Finally, 10 stable structures were reoptimized at the ωB97X-D/6-311++G (3df, 3pd) (for H, C, N and O atoms) + aug-cc-pVTZ-PP (for I atom) level of theory (Frisch, Pople and Binkley, 1984; Peterson, 2003; Chai and Head-Gordon, 2008; Elm and Kristensen, 2017) together with the calculations of vibrational frequencies. Notably, even though we try our best to search for the global minimum configurations of clusters considering the computational cost, saving 1000 local minima from the ABCluster search and selecting the lowest 100 cluster configurations based on PM7 may lead to the global minimum cluster being missed (Kurfman, Odbadrakh and Shields, 2021). Additionally, we manually constructed some potential stable clusters with multiple hydrogen/halogen bonding sites based on the chemical intuition. All quantum chemical calculations were performed using the Gaussian 09 package (Frisch et al., 2009) to identify the most stable conformations of each cluster.

Afterwards, the single-point energy correction was carried out by the RI-CC2/aug-cc-pVTZ (for H, C, N and O atoms) + aug-cc-pVTZ-PP with ECP28MDF (for I atom) using the Turbomole program (Ahlrichs et al., 1989), because of the good agreement between simulated results (e.g., the cluster formation rates) at the this theoretical level with the experimental results or field measurements through a random cancellation of errors (Almeida et al., 2013; Lu et al., 2020; Kürten et al., 2018). To assess the reliability of RI-CC2 method, we compared the simulated cluster formation rates obtained at  $\omega$ B97X-D/6-311++G(3df,3pd), RI-CC2/aug-cc-pVTZ, and DLPNO-CCSD(T)/aug-cc-pVTZ level of theory with the CLOUD experiment results (He et al., 2021) (Figure 1 and details can be found in Section S2). As shown in Figure 1, without performing single-point energy correction, the cluster formation rates simulated at  $\omega$ B97X-D/6-311++G(3df,3pd) level of theory (the diamond points) are significantly lower than the experimental results (the circular points). Therefore, we chose to perform the single-point correction to obtain simulated cluster formation rates that agree more with the experimental results. Compared to the results of DLPNO-CCSD(T) method, the simulated cluster formation rates based on RI-CC2 method are more consistent with the experimental results at T = 263 K. Moreover, at T = 283 K, the RI-CC2 results are closer to lower cluster formation rates from the experiments by less than two orders of magnitude. Considering that the results based on RI-CC2 method agree the most with experimental results

while saving computational resources, we finally chose the RI-CC2 method for single-point correction. It is important to note that this does not imply RI-CC2 results are inherently more accurate than those obtained using DLPNO-CCSD(T) method. We cautiously state that the choice of the RI-CC2 method in this study is due to its ability to effectively match the experimental results through a random cancellation of errors (details can be found in Section S2) while saving computational resources.

 $10^{1}$  $10^{-3}$ 10-7 - RI-CC2, 283 K RI-CC2, 263 K CLOUD, 283 K 10-11 CLOUD, 263 K DLPNO-CCSD, 283 K DLPNO-CCSD, 263 K wB97X-D, 283 K wB97X-D, 263 K  $10^{7}$  $10^{8}$  $10^{6}$ [HIO<sub>3</sub>] / molecules cm<sup>-3</sup>

**Figure 1.** The cluster formation rates (J, cm<sup>-3</sup> s<sup>-1</sup>) of HIO<sub>3</sub>-HIO<sub>2</sub> system obtained from experiment (CLOUD) and theoretical results at RI-CC2 and DLPNO-CCSD level of theory. The simulation was performed under the same conditions of [HIO<sub>3</sub>] =  $10^6 - 10^8$ , [HIO<sub>2</sub>] =  $2 \times 10^4 - 2 \times 10^6$ , T = 283 (red) / 263 (blue) K, and CS =  $2.2 \times 10^{-3}$  s<sup>-1</sup>. The circles represent the experimental results, the squares represent the theoretical results at RI-CC2/aug-cc-pVTZ (for H, C, N and O atoms) + aug-cc-pVTZ-PP with ECP28MDF (for I atom) level of theory, the triangles represent the theoretical results at DLPNO-CCSD(T)/aug-cc-pVTZ (for H, C, N and O atoms) + aug-cc-pVTZ-PP with ECP28MDF (for I atom) level of theory, and the diamonds represent the theoretical results at ωB97X-D/6-311++G(3df,3pd) (for H, C, N and O atoms) + aug-cc-pVTZ-PP with ECP28MDF (for I atom) level of theory.

In the present study, the Gibbs free energy of formation ( $\triangle G$ , kcal mol<sup>-1</sup>) of clusters was calculated as:

$$\Delta G = \Delta E_{\text{RI-CC2}} + \Delta G_{\text{thermal}}^{\omega B97X-D}$$

where  $\Delta E_{RI-CC2}$  is the electronic contribution obtained at the RI-CC2/aug-cc-pVTZ (for H, C, N and O atoms) + aug-cc-pVTZ-PP with ECP28MDF (for I atom) level of theory, and  $\Delta G_{thermal}^{\omega B97X-D}$  is the thermal contribution calculated at the  $\omega B97X-D/6-311++G(3df,3pd)$  (for H, C, N and O atoms) + aug-cc-pVTZ-PP with ECP28MDF (for I atom) level of theory.

## 2.2 Atmospheric Cluster Dynamics Code (ACDC) simulations

135

140

145

150

155

In order to investigate the effect of DMA on HIO<sub>3</sub>-HIO<sub>2</sub> nucleation in marine areas, a series of ACDC simulations (McGrath et al., 2012) were performed under atmospheric conditions corresponding to mid-latitudes coastal and high-latitudes polar regions. By solving the birth-death equation, the ACDC simulations can obtain the cluster formation rates and formation pathways of clusters using the MATLAB program (Shampine and Reichelt, 1997). The birth-death equation can be written as follows:

$$\frac{dc_{i}}{dt} = \frac{1}{2} \sum_{i < i} \beta_{j,(i-j)} c_{j} c_{i-j} + \sum_{i} \gamma_{(i+j) \to i} c_{i+j} - \sum_{i} \beta_{i,j} c_{i} c_{j} - \frac{1}{2} \sum_{i < i} \gamma_{i \to j} c_{i} + Q_{i} - S_{i}$$

where  $c_i$  is the concentration of cluster i,  $\beta_{i,j}$  is the collision coefficient between cluster i and cluster j,  $\gamma_{(i+j)\to i}$  is the evaporation coefficient of the cluster (i+j) evaporating into cluster i and cluster j,  $Q_i$  is the external source term of cluster i, and  $S_i$  is the potential sink term for cluster i.

The collision coefficient  $\beta_{i,j}$  can be written as:

$$\beta_{i,j} = \left(\frac{3}{4\pi}\right)^{\frac{1}{6}} \left(\frac{6k_{\rm B}T}{m_i} + \frac{6k_{\rm B}T}{m_j}\right)^{\frac{1}{2}} \left(V_i^{\frac{1}{3}} + V_j^{\frac{1}{3}}\right)^2$$

where  $k_B$  is the Boltzmann constant, T is the temperature,  $m_i$  is the mass of cluster i, and  $V_i$  is the van der Waals volume of cluster i, which is calculated by the improved Marching Tetrahedra (MT) approach (Lu and Chen, 2012b) using Multiwfn 3.7 program (Lu and Chen, 2012a).

The evaporation coefficient  $\gamma_{(i+j)\to i}$  of the cluster was obtained from the collision coefficient and the specific balance between cluster formation via the collision and cluster loss via the evaporation:

$$\gamma_{(i+j)\to i} = \beta_{i,j} c_{\text{ref}} \exp(\frac{\Delta G_{i+j} - \Delta G_i - \Delta G_j}{k_{\text{B}} T})$$

where  $c_{\text{ref}}$  is the monomer concentration under the reference pressure of 1 atm, and  $\Delta G_i$  is the Gibbs free energy of the formation of cluster i.

The formation of clusters is accompanied by the competition between collision and evaporation. The clusters with a collision frequency higher than the total evaporation frequency ( $\beta c/\Sigma \gamma > 1$ ) are considered to be stable in the perspective of nucleation kinetics. The detailed collision and total evaporation frequencies of the HIO<sub>3</sub>-HIO<sub>2</sub>-DMA system at all simulated temperatures and condensation sinks are listed in Tables S1-S4. The boundary conditions of the ACDC simulations are closely related to the ratio of the collision frequency between the clusters and monomer molecules at the concentration c to the total evaporation frequency of clusters. Moreover, the size of clusters in the simulation system also affects the accuracy of the simulation results (Figure S1). We will discuss the issues related to the size of clusters and the settings of boundary clusters in detail in Section S3 of Supporting Information.

#### 3 Results

160

165

170

175

180

185

190

# 3.1 Cluster stable configurations

The most stable configurations of the HIO<sub>3</sub>-HIO<sub>2</sub>-DMA ternary clusters at the  $\omega$ B97X-D/6-311++G(3df,3pd) (for H, C, N, and O atoms) + aug-cc-pVTZ-PP with ECP28MDF (for I atom) level of theory are shown in Figure 2. The structures of the HIO<sub>2</sub>-DMA clusters can be found in Figure S3 of the Supporting Information, and the cartesian coordinates of all HIO<sub>3</sub>-HIO<sub>2</sub>-DMA and HIO<sub>2</sub>-DMA clusters are shown in Table S7. The electrostatic potential (ESP) distribution (details in Section S4 of Supporting Information) showed that the -NH group of DMA molecules can act as both donor and acceptor of non-covalent interactions. Hence, DMA can form stable ternary clusters through the space network formed by HBs and XBs. Moreover, acid-base proton transfer can be found in all ternary clusters except for the (HIO<sub>3</sub>)<sub>1</sub>(HIO<sub>2</sub>)<sub>2</sub>(DMA)<sub>1</sub> and (HIO<sub>3</sub>)<sub>1</sub>(HIO<sub>2</sub>)<sub>3</sub>(DMA)<sub>2</sub> clusters. It has been shown in the previous study on HIO<sub>3</sub>-DMA and HIO<sub>3</sub>-HIO<sub>2</sub> systems that acid-base proton transfer occurred between HIO<sub>3</sub> and HIO<sub>2</sub>/DMA (Zhang et al., 2022a; Ning et al., 2022; Liu et al., 2023). The gas-phase basicity of DMA is strong (896.5 kJ mol<sup>-1</sup>) (Yang et al., 2018). Hence, DMA is capable to efficiently stabilize acidic precursors through acid-base interactions. Moreover, amphoteric HIO<sub>2</sub> molecules, the acid dissociation constant (pK<sub>a</sub>) of which is 6.0 (Schmitz, 2008), can also exhibit base-like behavior in the neutral nucleation process of HIO<sub>3</sub>-HIO<sub>2</sub> (Zhang et al., 2022a; Liu et al., 2023). This indicates that DMA may play a role similar to HIO<sub>2</sub> in the neutral nucleation process driven by HIO<sub>3</sub>.

In order to assess the effect of DMA on the proton transfer process, the analysis of the proton transfer was performed based on the change of bond length at corresponding positions that conduct acid-base reaction. The number of proton transfer between different precursors in ternary clusters and the total number of proton transfer are summarized in Table S8. As shown in Table S8, among most of the ternary clusters, HIO<sub>3</sub> will preferentially interact with DMA, which possesses strong basicity, in the process of proton transfer. Afterwards, the remaining HIO3 can perform proton transfer with the amphoteric HIO2, which can also exhibit base-like behavior under this circumstance. It is worth noting that, in terms of the stability (evaluated by  $\Delta G$ ) of clusters, the proton transfer plays a crucial role. Taking two 3-molecule clusters,  $(HIO_3)_2(HIO_2)_1$  ( $\Delta G = -30.05 \text{ kcal mol}^{-1}$ ) and  $(HIO_3)_1(HIO_2)_1(DMA)_1$  ( $\Delta G = -35.19 \text{ kcal mol}^{-1}$ ), as an example, we observed that the (HIO<sub>3</sub>)<sub>2</sub>(HIO<sub>2</sub>)<sub>1</sub> cluster with higher energy is formed through three XBs and one HB, while (HIO<sub>3</sub>)<sub>1</sub>(HIO<sub>2</sub>)<sub>1</sub>(DMA)<sub>1</sub> cluster with lower energy is formed through three HBs after proton transfer. Additionally, when the number of proton transfers is the same, clusters with more halogen bonds formed by  $HIO_2$  generally have lower  $\Delta G$ , which can be seen from  $(HIO_3)_1(HIO_2)_2(DMA)_1$  ( $\Delta G = -50.07$  kcal mol<sup>-1</sup>, formed by three XBs and two HBs) and  $(HIO_2)_4$  ( $\Delta G = -58.08$  kcal mol<sup>-1</sup>, formed by four XBs) clusters. Similar results can also be observed in other ternary clusters. As for the water (H2O) molecules, they are indispensable in the formation process of marine aerosols. However, previous studies have indicated that H<sub>2</sub>O contributes less significantly to strong acid-base systems dominated by proton transfer, such as the H<sub>2</sub>SO<sub>4</sub>-DMA system (Kürten et al., 2018; Olenius et al., 2017; Liu et al., 2021b). The HIO<sub>3</sub>-HIO<sub>2</sub>-DMA system exhibits clustering pattern similar to the H<sub>2</sub>SO<sub>4</sub>-DMA system, with proton transfer processes in almost all ternary clusters. Hence, we speculate that the contribution of H<sub>2</sub>O to the HIO<sub>3</sub>-HIO<sub>2</sub>-DMA system is relatively weak similar with contribution of H<sub>2</sub>O to the H<sub>2</sub>SO<sub>4</sub>-DMA system. In addition, considering that the introduction of hydrated clusters requires large amount of additional quantum chemical calculations, which are time-consuming in current workflow, the impact of H<sub>2</sub>O is not considered in the present study.

195

200

205

210

215

In summary, the structural analysis shows that DMA can form stable clusters with iodine oxoacids via HBs, XBs and proton transfer, laying the foundation for promoting HIO<sub>3</sub>-HIO<sub>2</sub> nucleation. Moreover, DMA can preferentially accept the proton from HIO<sub>3</sub> in the most stable configurations of HIO<sub>3</sub>-HIO<sub>2</sub>-DMA clusters, while the amphoteric HIO<sub>2</sub> can also exhibit similar behavior.

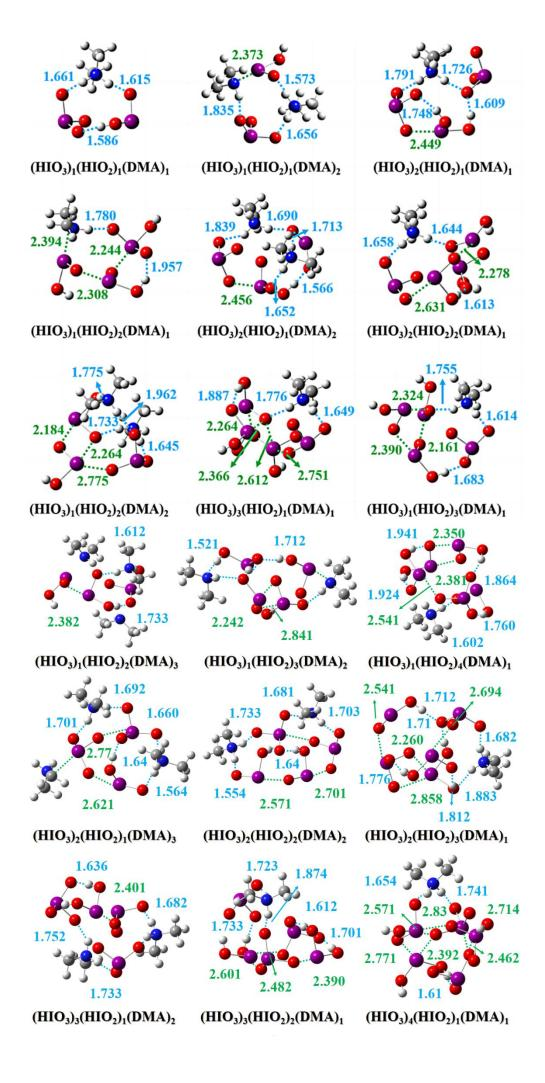


Figure 2. The most stable structures of HIO<sub>3</sub>-HIO<sub>2</sub>-DMA clusters identified at the ωB97X-D/6-311++G(3df,3pd) (for H, C, N and O atoms) + aug-cc-pVTZ-PP with ECP28MDF (for I atom) level of theory. The white, grey, blue, red, and purple balls represent the H, C, N, O, and I atoms, respectively. The hydrogen bonds and halogen bonds are shown in blue and green dashed lines, respectively. The values of bond lengths are given in Å.

## 3.2 Cluster formation pathways

225

230

235

To further study the kinetic behavior of DMA in nucleation process, the ACDC was used to simulate the nucleation pathways under marine atmospheric conditions. Firstly, a specific simulation was performed under atmospheric conditions reported in Zhejiang, an intersection of high [DMA] pollution air masses and marine iodine air masses at the east coast of China (Zhu et al., 2019; Zhang et al., 2023). The main cluster formation pathways, which contributes more than 5% to the total cluster formation rates, at [HIO<sub>3</sub>] of  $1.0 \times 10^7$  molecules cm<sup>-3</sup>, [HIO<sub>2</sub>] of  $2.0 \times 10^5$  molecules cm<sup>-3</sup> and T = 293 K are shown in Figure 3. The average condensation sink (CS) was estimated and set to be  $1.0 \times 10^{-2}$  s<sup>-1</sup> for polluted coastal regions (Ning et al., 2022). In Figure 3, we present the simulation results under three different [DMA] conditions ([DMA] = 0, 0.04, and 4 pptv) to evaluate the influence of DMA on the nucleation process of iodine oxoacids. As shown in Figure 3, with the increase of [DMA], the cluster formation pathways in the simulated system undergo continuous changes. The primary pathway shifts from the binary HIO<sub>3</sub>-HIO<sub>2</sub> pathway to the ternary HIO<sub>3</sub>-HIO<sub>2</sub>-DMA pathway, and further to the binary HIO<sub>3</sub>-DMA pathway. Hence, DMA might be involved in the nucleation process of the HIO<sub>3</sub>-HIO<sub>2</sub> system in coastal regions, especially in those regions affected by high [DMA].

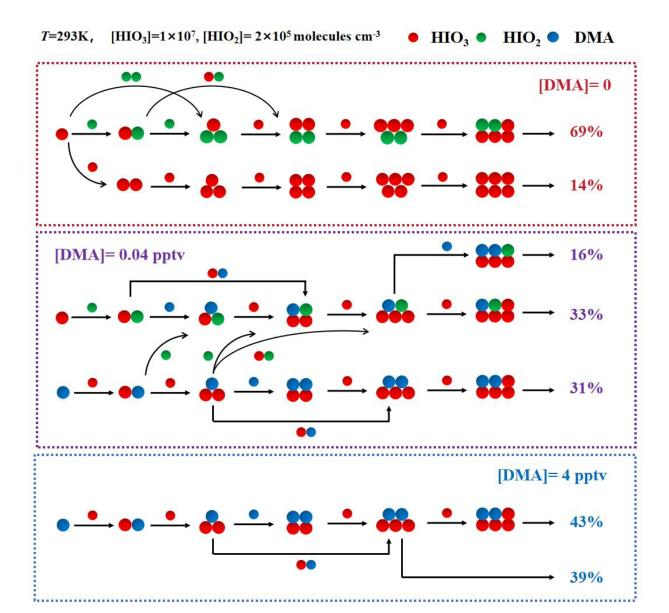


**Figure 3.** The cluster formation pathways and the contribution of main pathways to the total cluster formation rates under field conditions of Zhejiang at [HIO<sub>3</sub>] of  $1.0 \times 10^7$  molecules cm<sup>-3</sup>, [HIO<sub>2</sub>] of  $2.0 \times 10^5$  molecules cm<sup>-3</sup>, [DMA] of 0 (red), 0.04 (purple), and 4 (blue) pptv, T = 293 K, and CS =  $1.0 \times 10^{-2}$  s<sup>-1</sup>. The red, green, and blue balls represent the HIO<sub>3</sub>, HIO<sub>2</sub>, and DMA molecules, respectively.

The simulated nucleation pathway under the specific condition has proved the participation of DMA in  $HIO_3$ - $HIO_2$  nucleation. However, since  $HIO_x$  (x=2,3) and DMA originate from different sources, the concentrations of precursors should be changed to better represent the situation of regions with different iodine and amine emission intensities. Therefore, to further study the involvement of DMA in nucleation pathways under various oceanic atmospheric conditions, the contribution of the main cluster formation pathways at different concentrations are simulated and the results are shown in Figure 4. It is worth noting that the concentration of  $HIO_2$  changes together with that of  $HIO_3$  from low to high since  $HIO_2$  and  $HIO_3$  are homologous iodine species. The ratio of  $[HIO_3]$  to  $[HIO_2]$  is about 20 to 100 depending on the concentration of iodine vapor (Yu et al., 2019; Baccarini et al., 2020; Rong et al., 2020; Xia et al., 2020; He et al., 2021; Sipilä et al., 2016). The ratio used in Figure 4 was 50 according to the former field observations in Mace Head (Sipilä et al., 2016) and the other results obtained from two different ratios (20 and 100) of  $[HIO_3]$  and  $[HIO_2]$  can be seen from the Section S5 of Supporting Information.

As can be seen from Figure 4, the contribution of DMA to the nucleation increases with [DMA] rising from 10<sup>-3</sup> to 1 pptv, and the dominating mechanism varies similarly with Figure 3 from HIO<sub>3</sub>-HIO<sub>2</sub> nucleation to HIO<sub>3</sub>-HIO<sub>2</sub>-DMA nucleation and then to HIO<sub>3</sub>-DMA nucleation. Moreover, combining Figures S4 and S5, an opposite trend in the dominant mechanism becomes apparent with the increase of [HIO<sub>2</sub>]. Specifically, the primary nucleation mechanism shifts from HIO<sub>3</sub>-DMA to HIO<sub>3</sub>-HIO<sub>2</sub>-DMA, or from HIO<sub>3</sub>-HIO<sub>2</sub>-DMA to HIO<sub>3</sub>-HIO<sub>2</sub> as [HIO<sub>2</sub>] increase. Notably, the HIO<sub>3</sub>-HIO<sub>2</sub>-DMA ternary mechanism is more significant when [HIO<sub>2</sub>] and [DMA] are similar. In contrast, when DMA (HIO<sub>2</sub>) is much more abundant than HIO2 (DMA), the pathways are overwhelmingly dominated by rapid binary nucleation involving HIO3 and DMA (HIO<sub>2</sub>) with higher concentration. This phenomenon may be attributed to the similar stabilizing effects of DMA and HIO<sub>2</sub> on HIO<sub>3</sub> nucleation, where the component with a higher concentration plays a more significant role. Consequently, the component with a lower concentration exerts less influence, primarily due to the limited availability of HIO<sub>3</sub>. This indicates that when [DMA] reaches 10<sup>-1</sup> to 1 pptv, the proportion of DMA-containing pathways will approach 100% (Figure 4), indicating significant involvement of DMA on HIO3-HIO2 system. As mentioned in the introduction, marine regions are not lacking in high-intensity sources of DMA, especially in polluted coastal areas. However, currently reported experiments and model simulations seem to have not yet focused on the ternary HIO<sub>3</sub>-HIO<sub>2</sub>-DMA mechanism. Therefore, in the next section, we will evaluate the nucleation ability of the newly proposed HIO<sub>3</sub>-HIO<sub>2</sub>-DMA mechanism through comparison with classical nucleation mechanism or observation results to comprehensively assess the environmental significance of HIO<sub>3</sub>-HIO<sub>2</sub>-DMA mechanism in the broad marine regions.

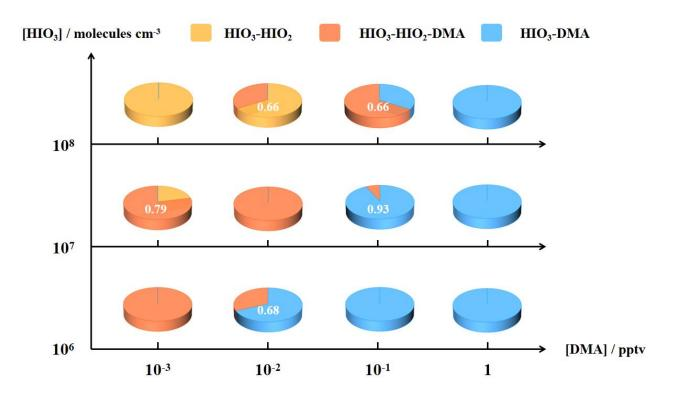


**Figure 4.** The contribution of main nucleation pathways at different concentrations of precursors. [HIO<sub>3</sub>] =  $10^6$  -  $10^8$  molecules cm<sup>-3</sup>, [HIO<sub>2</sub>] =  $2.0 \times 10^4$  -  $2.0 \times 10^6$  molecules cm<sup>-3</sup> and [DMA] =  $10^{-3}$  - 1 pptv. The simulated temperature and condensation sink are 283 K and  $2.0 \times 10^{-3}$  s<sup>-1</sup> as typical values for oceanic atmosphere. The proportion of the contribution of HIO<sub>3</sub>-HIO<sub>2</sub>, HIO<sub>3</sub>-HIO<sub>2</sub>-DMA, and HIO<sub>3</sub>-DMA are shown in yellow, orange, and blue, respectively.

# 3.3 Cluster formation rates

255

260

265

270

275

280

The cluster formation pathway showed that DMA may significantly participate in  $HIO_3$ - $HIO_2$  nucleation. However, the influence of DMA on the cluster formation rates (J, cm<sup>-3</sup> s<sup>-1</sup>) of the  $HIO_3$ - $HIO_2$  nucleation is still unknown. To evaluate the

influence of DMA on HIO<sub>3</sub>-HIO<sub>2</sub> system and the environmental significance of HIO<sub>3</sub>-HIO<sub>2</sub>-DMA system, we compared the *J* of HIO<sub>3</sub>-HIO<sub>2</sub> (red), HIO<sub>3</sub>-HIO<sub>2</sub>-DMA (purple), HIO<sub>3</sub>-HIO<sub>2</sub>-H<sub>2</sub>SO<sub>4</sub> (yellow), HIO<sub>3</sub>-HIO<sub>2</sub>-MSA (pink), and H<sub>2</sub>SO<sub>4</sub>-DMA (blue) systems under the simulated conditions of typical marine and polar regions. The results of HIO<sub>3</sub>-HIO<sub>2</sub>-H<sub>2</sub>SO<sub>4</sub> (Zu et al., 2024) and HIO<sub>3</sub>-HIO<sub>2</sub>-MSA systems (https://doi.org/10.5194/egusphere-2023-2084) were obtained from former studies at the same level of theory with HIO<sub>3</sub>-HIO<sub>2</sub>-DMA system. The configurations of H<sub>2</sub>SO<sub>4</sub>-DMA clusters were obtained from the Atmospheric Cluster Database (ACDB) (Elm, 2019). Subsequently, geometric optimizations and frequency calculations were performed at the same (ωB97X-D/6-311++G(3df,3pd)) level of theory with HIO<sub>3</sub>-HIO<sub>2</sub>-DMA system. Notably, we believe that the influence of other mechanisms (HIO<sub>3</sub>-HIO<sub>2</sub>-A, etc.) is widespread and significant. However, due to the lack of available data, other mechanisms are not discussed in this study and will be considered in further studies.

285

290

295

300

305

310

315

320

325

The Zhejiang region experiences the frequent NPF events, closely associated with a high-intensity iodine-driven nucleation process (Yu et al., 2019). However, our simulation results under the conditions of Zhejiang (Xia et al., 2020; Yu et al., 2019) indicate that relying solely on HIO<sub>3</sub>-HIO<sub>2</sub> nucleation (red curve in Figure 5(a)) appears insufficient to explain the rapid formation rates of ambient environment (gray shaded area). It is noteworthy that the NPF events in the local area is found to be influenced not only by marine components but also by urban pollutants (Zhu et al., 2019; Liu et al., 2022). During polluted periods, the emission capacity of gas-phase DMA is exceptionally strong, and high concentrations of DMA can further enhance the J of HIO<sub>3</sub>-HIO<sub>2</sub>, resulting in a significant enhancement of up to  $10^8$  times at [DMA] = 4 pptv. Notably, the increase of the concentrations of  $HIO_2$  and DMA can both enhance the J to match the field observations, indicating that HIO2 and DMA molecules exhibit a synergistic effect on HIO3 nucleation, which may have significant contributions to NPF events in the polluted coastal areas where marine iodine species intersect with high concentrations of DMA. Moreover, the urban pollution also leads to an abundant concentration of gas-phase H<sub>2</sub>SO<sub>4</sub>. This renders the impact of the HIO<sub>3</sub>-HIO<sub>2</sub>-H<sub>2</sub>SO<sub>4</sub> and H<sub>2</sub>SO<sub>4</sub>-DMA mechanisms non-negligible. As shown in Figure 5(a), the simulated J of H<sub>2</sub>SO<sub>4</sub>-DMA and HIO<sub>3</sub>-HIO<sub>2</sub>-H<sub>2</sub>SO<sub>4</sub> systems (blue dashed line) is about one or four orders of magnitude lower than that of HIO<sub>3</sub>-HIO2-DMA system, respectively. This indirectly indicates that the HIO3-HIO2 system promoted by DMA possesses remarkable nucleation ability and might make unexpected contributions in specific regions, thereby providing an explanation for some missing fluxes of particles in the atmosphere.

In contrast, the results from the Mace Head region present a different situation. Previous studies have demonstrated that local nucleation is primarily driven by high concentrations of HIO<sub>3</sub> (Sipilä et al., 2016). The simulated results showed that the *J* of HIO<sub>3</sub>-HIO<sub>2</sub> system can reach up to levels of 10<sup>4</sup> cm<sup>-3</sup> s<sup>-1</sup>, which is consistent with the upper limit of formation rates reported in the field observation (Sipilä et al., 2016). Furthermore, we evaluated the potential impact of DMA and other precursors on the *J* of HIO<sub>3</sub>-HIO<sub>2</sub> system based on the concentrations from model simulations or gas-phase measurements reported at Mace Head (Yu and Luo, 2014; Sipilä et al., 2016). The results indicate that DMA can promote the *J* significantly only at lower iodine concentrations. As the increases of iodine oxoacids, the *J* of HIO<sub>3</sub>-HIO<sub>2</sub>-DMA system gradually approaches that of HIO<sub>3</sub>-HIO<sub>2</sub> system, indicating a less significant enhancement by DMA. Similar patterns about the enhancement by H<sub>2</sub>SO<sub>4</sub> and MSA can also be shown. This indicates that in primitive regions with abundant iodine sources, even if the precursors (DMA, H<sub>2</sub>SO<sub>4</sub>, and MSA) can reach the high concentrations used in the simulation in this study, their corresponding enhancement is limited. The primary nucleation mechanism is likely to be the HIO<sub>3</sub>-HIO<sub>2</sub> mechanism, which is supported by the on-site measurements of the components of nanoparticles (Sipilä et al., 2016).

Recent research has shown that the ice-influenced ocean may also be important sources of DMA (Dall'Osto et al., 2017; Dall'Osto et al., 2019). Hence, we also evaluate the environmental significance of HIO<sub>3</sub>-HIO<sub>2</sub>-DMA system in the ice-covered polar regions. As shown in Figure 5(c), we performed a simulation under the conditions of Aboa station. The simulation results indicate that HIO<sub>3</sub>-HIO<sub>2</sub>-H<sub>2</sub>SO<sub>4</sub> and H<sub>2</sub>SO<sub>4</sub>-DMA are more efficient nucleation mechanisms than HIO<sub>3</sub>-HIO<sub>2</sub>-DMA system in the local area. Moreover, the simulated *J* of HIO<sub>3</sub>-HIO<sub>2</sub>-DMA system is also slightly lower than the formation rates (0.05 - 0.12 cm<sup>-3</sup> s<sup>-1</sup>) of ion-induced H<sub>2</sub>SO<sub>4</sub>-A system reported by field observations (Jokinen et al., 2018). Hence, due to the overall lower concentrations of iodine and amine components, the nucleation process is predominantly driven by H<sub>2</sub>SO<sub>4</sub> molecules. This suggests that in regions with scarce iodine and amine sources, the contribution of the DMA-enhanced HIO<sub>3</sub>-HIO<sub>2</sub> mechanism to the particle formation is limited. In contrast, in the Marambio region with relatively abundant DMA and scarce iodine oxoacids (Quéléver et al., 2022; Wang et al., 2023), HIO<sub>3</sub>-HIO<sub>2</sub>-DMA system

may also have significant contributions [Figure 5(d)]. The [HIO<sub>3</sub>] used in the simulation is still about an order of magnitude lower than [H<sub>2</sub>SO<sub>4</sub>] and [MSA]. However, [DMA] is about an order of magnitude higher than that in the Aboa region. In this case, the *J* of HIO<sub>3</sub>-HIO<sub>2</sub> system is significantly enhanced for more than 10<sup>3</sup>-fold by the relatively abundant DMA. Compared to the acidic components such as H<sub>2</sub>SO<sub>4</sub> and MSA, DMA elevates the *J* of the HIO<sub>3</sub>-HIO<sub>2</sub> system to the range of 10<sup>-1</sup> to 10<sup>1</sup> cm<sup>-3</sup> s<sup>-1</sup>, matching the field observation results, while [DMA] is only one-tenth of [H<sub>2</sub>SO<sub>4</sub>] and [MSA]. This indicates that, considering nucleation ability, the enhancement effect of DMA on the HIO<sub>3</sub>-HIO<sub>2</sub> system may be superior to H<sub>2</sub>SO<sub>4</sub> and MSA, which we speculate that is likely related to the base stabilization effect of DMA within acidic clusters. Additionally, our results demonstrate that the nucleation ability of HIO<sub>3</sub>-HIO<sub>2</sub>-DMA is stronger than that of H<sub>2</sub>SO<sub>4</sub>-DMA. This means that the HIO<sub>3</sub>-HIO<sub>2</sub>-DMA ternary mechanism may be an important contributor to iodine-containing particles, especially in regions where there are sufficient iodine and amine sources.

In summary, the results show that HIO<sub>3</sub>-HIO<sub>2</sub>-DMA ternary nucleation mechanism may have significant contributions to the formation of nanoparticles, especially in those regions with abundant iodine and amine sources. This previously overlooked mechanism may provide an explanation for some missing fluxes of atmospheric iodine particles. Moreover, the observed formation rates in the field can result from multiple rapid nucleation systems or may be solely attributed to a specific system, depending significantly on the variations of precursor concentrations in different regions. The nucleation process in real atmosphere is complex. Hence, the simulation of scenarios where various components participate simultaneously is needed in the future study to accurately assess the roles of different components such as H<sub>2</sub>SO<sub>4</sub>, MSA, A, and DMA in the iodine oxoacids nucleation. This may contribute to a fundamental understanding of atmospheric particle formation, providing a comprehensive insight into the entire evolution process of atmospheric aerosols.

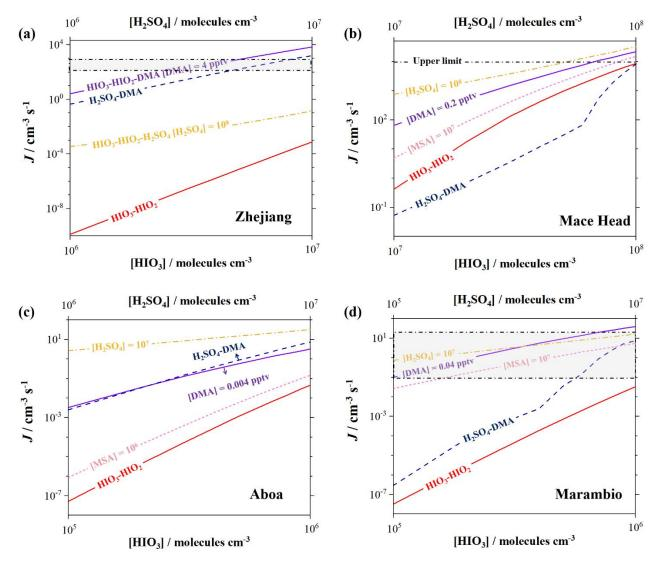


Figure 5. The cluster formation rates (J, cm<sup>-3</sup> s<sup>-1</sup>) of HIO<sub>3</sub>-HIO<sub>2</sub> (red), HIO<sub>3</sub>-HIO<sub>2</sub>-DMA (purple), HIO<sub>3</sub>-HIO<sub>2</sub>-

 $H_2SO_4(yellow)$ ,  $HIO_3$ - $HIO_2$ -MSA (pink), and  $H_2SO_4$ -DMA (blue) systems under the simulated conditions of (a) Zhejiang: [HIO<sub>3</sub>] =  $10^6$  -  $10^7$ , [HIO<sub>2</sub>] =  $2 \times 10^4$  -  $2 \times 10^5$ , [H<sub>2</sub>SO<sub>4</sub>] =  $10^6$  -  $10^8$  molecules cm<sup>-3</sup>, and [DMA] = 4 pptv, (b) Mace Head: [HIO<sub>3</sub>] =  $10^7$  -  $10^8$ , [HIO<sub>2</sub>] =  $2 \times 10^5$  -  $2 \times 10^6$ , [H<sub>2</sub>SO<sub>4</sub>] =  $10^7$  -  $10^8$ , [MSA] =  $10^7$  molecules cm<sup>-3</sup>, and [DMA] = 0.2 pptv, (c) Aboa: [HIO<sub>3</sub>] =  $10^5$  -  $10^6$ , [HIO<sub>2</sub>] =  $2 \times 10^3$  -  $2 \times 10^4$ , [H<sub>2</sub>SO<sub>4</sub>] =  $10^6$  -  $10^7$ , [MSA] =  $10^6$  molecules cm<sup>-3</sup>, and [DMA] = 0.004 pptv, and (d) Marambio: [HIO<sub>3</sub>] =  $10^5$  -  $10^6$ , [HIO<sub>2</sub>] =  $2 \times 10^3$  -  $2 \times 10^4$ , [H<sub>2</sub>SO<sub>4</sub>] =  $10^5$  -  $10^7$ , [MSA] =  $10^7$  molecules cm<sup>-3</sup>, and [DMA] = 0.04 pptv. The shaded area (grey) represents the actual nucleation rates observed locally.

## 4 Atmospheric significance and conclusion

The present study investigated the iodine oxoacids nucleation enhanced by DMA under broad oceanic atmospheric conditions by the quantum chemical calculations combined with ACDC simulations. As a basic precursor to stabilize acid, DMA can form the stable ternary clusters with HIO<sub>3</sub> and HIO<sub>2</sub>, in which DMA can preferentially accept the proton from HIO<sub>3</sub>. Kinetically, the participation of DMA in the participation of DMA in the cluster formation pathways of iodine oxoacids system be significant at 10<sup>-1</sup> - 1 pptv level of [DMA]. Furthermore, DMA can enhance the cluster formation rates of the HIO<sub>3</sub>-HIO<sub>2</sub> system in marine and polar regions near DMA sources for more than 10<sup>3</sup>-fold. Compared to the classical nucleation mechanism, the HIO<sub>3</sub>-HIO<sub>2</sub>-DMA mechanism exhibits strong nucleation ability, worthy of consideration as a promising mechanism in marine and polar regions rich in amine sources. The nucleation mechanism in real atmosphere is more complex and may result from multiple rapid nucleation systems, depending significantly on the variations of precursor concentrations in different regions. Hence, there is an urgent need to develop atmospheric models that comprehensively consider the coupling effects of multiple mechanisms.

## Data availability

355

360

365

375

380

390

The data in this article can be available from the corresponding author upon request (<u>lingliu@bit.edu.cn</u> and <u>zhangxiuhui@bit.edu.cn</u>).

## **Supplement**

The supplement related to this article is available online at: XXXXXXXX.

#### **Author contributions**

XZ designed and supervised the research. HZ performed the quantum chemical calculations and the ACDC simulations. HZ and LL analyzed data. HZ, LL and XZ wrote the paper. XZ, LL, BC, and YL reviewed and edited the paper. All authors commented on the paper.

## **Competing interests**

The contact author has declared that neither they nor their co-authors have any competing interests.

## Disclaimer

Publisher's note: Copernicus Publications remains neutral with regard to jurisdictional claims in published maps and institutional affiliations.

#### Acknowledgements

We acknowledge the National Supercomputing Center in Shenzhen for providing the computational resources and the Turbomole program.

#### **Financial support**

This work is supported by the National Science Fund for Distinguished Young Scholars (grant no. 22225607), the National

## References

- Ahlrichs, R., Bar, M., Horn, H. and Kolmel, C.: Electronic-structure calculations on workstation computers the program system turbomole., Chemical Physics Letters, 162, 165-169, 1989.
- Almeida, J., Schobesberger, S., Kürten, A., Ortega, I. K., Kupiainen-Määttä, O., Praplan, A. P., Adamov, A., Amorim, A.,
  Bianchi, F., Breitenlechner, M., David, A., Dommen, J., Donahue, N. M., Downard, A., Dunne, E., Duplissy, J.,
  Ehrhart, S., Flagan, R. C., Franchin, A., Guida, R., Hakala, J., Hansel, A., Heinritzi, M., Henschel, H., Jokinen, T.,
  Junninen, H., Kajos, M., Kangasluoma, J., Keskinen, H., Kupc, A., Kurtén, T., Kvashin, A. N., Laaksonen, A.,
  Lehtipalo, K., Leiminger, M., Leppa, J., Loukonen, V., Makhmutov, V., Mathot, S., McGrath, M. J., Nieminen, T.,
  Olenius, T., Onnela, A., Petäjä, T., Riccobono, F., Riipinen, I., Rissanen, M., Rondo, L., Ruuskanen, T., Santos, F.
  D., Sarnela, N., Schallhart, S., Schnitzhofer, R., Seinfeld, J. H., Simon, M., Sipilä, M., Stozhkov, Y., Stratmann, F.,
  Tomé, A., Tröstl, J., Tsagkogeorgas, G., Vaattovaara, P., Viisanen, Y., Virtanen, A., Vrtala, A., Wagner, P. E.,
  Weingartner, E., Wex, H., Williamson, C., Wimmer, D., Ye, P. L., Yli-Juuti, T., Carslaw, K. S., Kulmala, M., Curtius,
  J., Baltensperger, U., Worsnop, D. R., Vehkamäki, H. and Kirkby, J.: Molecular understanding of sulphuric acidamine particle nucleation in the atmosphere, Nature, 502, 359-+, <a href="http://doi.org/10.1038/nature12663">http://doi.org/10.1038/nature12663</a>, 2013.
- Baccarini, A., Karlsson, L., Dommen, J., Duplessis, P., Vüllers, J., Brooks, I. M., Saiz-Lopez, A., Salter, M., Tjernström, M., Baltensperger, U., Zieger, P. and Schmale, J.: Frequent new particle formation over the high Arctic pack ice by enhanced iodine emissions, Nature Communications, 11, http://doi.org/10.1038/s41467-020-18551-0, 2020.
  - Chai, J.-D. and Head-Gordon, M.: Long-range corrected hybrid density functionals with damped atom-atom dispersion corrections, Physical Chemistry Chemical Physics, 10, 6615-6620, 2008.
- Chen, D. H., Shen, Y. J., Wang, J. T., Gao, Y., Gao, H. W. and Yao, X. H.: Mapping gaseous dimethylamine, trimethylamine, ammonia, and their particulate counterparts in marine atmospheres of China's marginal seas Part 1: Differentiating marine emission from continental transport, Atmospheric Chemistry and Physics, 21, 16413-16425, http://doi.org/10.5194/acp-21-16413-2021, 2021.
- Chen, D. P., Li, D. F., Wang, C. W., Liu, F. Y. and Wang, W. L.: Formation mechanism of methanesulfonic acid and ammonia clusters: A kinetics simulation study, Atmospheric Environment, 222, <a href="http://doi.org/10.1016/j.atmosenv.2019.117161">http://doi.org/10.1016/j.atmosenv.2019.117161</a>, 2020a.
  - Chen, D. P., Li, D. F., Wang, C. W., Luo, Y., Liu, F. Y. and Wang, W. L.: Atmospheric implications of hydration on the formation of methanesulfonic acid and methylamine clusters: A theoretical study, Chemosphere, 244, <a href="http://doi.org/10.1016/j.chemosphere.2019.125538">http://doi.org/10.1016/j.chemosphere.2019.125538</a>, 2020b.
- Corral, A. F., Choi, Y., Collister, B. L., Crosbie, E., Dadashazar, H., DiGangi, J. P., Diskin, G. S., Fenn, M., Kirschler, S. and Moore, R. H. J. E. S. A.: Dimethylamine in cloud water: a case study over the northwest Atlantic Ocean, Environmental Science: Atmospheres, 2, 1534-1550, 2022.
- Dall'Osto, M., Airs, R. L., Beale, R., Cree, C., Fitzsimons, M. F., Beddows, D., Harrison, R. M., Ceburnis, D., O'Dowd, C., Rinaldi, M., Paglione, M., Nenes, A., Decesari, S. and Simó, R.: Simultaneous Detection of Alkylamines in the Surface Ocean and Atmosphere of the Antarctic Sympagic Environment, Acs Earth and Space Chemistry, 3, 854-+, <a href="http://doi.org/10.1021/acsearthspacechem.9b00028">http://doi.org/10.1021/acsearthspacechem.9b00028</a>, 2019.
  - Dall'Osto, M., Beddows, D. C. S., Tunved, P., Krejci, R., Ström, J., Hansson, H. C., Yoon, Y. J., Park, K. T., Becagli, S., Udisti, R., Onasch, T., O'Dowd, C. D., Simo, R. and Harrison, R. M.: Arctic sea ice melt leads to atmospheric new particle formation, Scientific Reports, 7, http://doi.org/10.1038/s41598-017-03328-1, 2017.
- Ehn, M., Vuollekoski, H., Petäjä, T., Kerminen, V. M., Vana, M., Aalto, P., de Leeuw, G., Ceburnis, D., Dupuy, R., O'Dowd, C. D. and Kulmala, M.: Growth rates during coastal and marine new particle formation in western Ireland, Journal of Geophysical Research-Atmospheres, 115, http://doi.org/10.1029/2010jd014292, 2010.
  - Elm, J.: Assessment of binding energies of atmospherically relevant clusters, Physical Chemistry Chemical Physics 15,

16442-16445, 2013.

470

- ---. An Atmospheric Cluster Database Consisting of Sulfuric Acid, Bases, Organics, and Water, Acs Omega, 4, 10965-10974, <a href="http://doi.org/10.1021/acsomega.9b00860">http://doi.org/10.1021/acsomega.9b00860</a>, 2019.
  - ---. Clusteromics I: Principles, Protocols, and Applications to Sulfuric Acid-Base Cluster Formation, Acs Omega, 6, 7804-7814, <a href="http://doi.org/10.1021/acsomega.1c00306">http://doi.org/10.1021/acsomega.1c00306</a>, 2021a.
- ---. Clusteromics II: Methanesulfonic Acid-Base Cluster Formation, Acs Omega, 6, 17035-17044, http://doi.org/10.1021/acsomega.1c02115, 2021b.
  - Elm, J. and Kristensen, K.: Basis set convergence of the binding energies of strongly hydrogen-bonded atmospheric clusters, Physical Chemistry Chemical Physics, 19, 1122-1133, <a href="http://doi.org/10.1039/c6cp06851k">http://doi.org/10.1039/c6cp06851k</a>, 2017.
  - Elm, J., Passananti, M., Kurtén, T. and Vehkamäki, H.: Diamines Can Initiate New Particle Formation in the Atmosphere, Journal of Physical Chemistry A, 121, 6155-6164, http://doi.org/10.1021/acs.jpca.7b05658, 2017.
- Facchini, M. C., Decesari, S., Rinaldi, M., Carbone, C., Finessi, E., Mircea, M., Fuzzi, S., Moretti, F., Tagliavini, E., Ceburnis, D. and O'Dowd, C. D.: Important Source of Marine Secondary Organic Aerosol from Biogenic Amines, Environmental Science & Technology, 42, 9116-9121, http://doi.org/10.1021/es8018385, 2008.
  - Frisch, M. J., Pople, J. A. and Binkley, J. S.: Self-consistent molecular orbital methods 25. Supplementary functions for Gaussian basis sets., Journal of Chemical Physics, 80, 3265-3269, 1984.
- Frisch, M. J., Trucks, G.W., Schlegel, H.B., Scuseria, G.E., Robb, M.A., Cheeseman, J.R., Scalmani, G., Barone, V., Mennucci, B., Petersson, G.A., Nakatsuji, H., Caricato, M., Li, X., Hratchian, H.P., Izmaylov, A.F., Bloino, J., Zheng, G., Sonnenberg, J.L., Hada,, M., E., M., Toyota, K., Fukuda, R., Hasegawa, J., Ishida, M., Nakajima, T., Honda,, Y., K., O., Nakai, H., Vreven, T., Montgomery, J.A., Peralta, J.E., Ogliaro, F., Bearpark, M., Heyd, J.J., Brothers, E., Kudin, K.N., Staroverov, V.N., Kobayashi, R.,, Normand, J., Raghavachari, K., Rendell, A., Burant, J.C., Iyengar, S.S., Tomasi, J.,, Cossi, M., Rega, N., Millam, J.M., Klene, M., Knox, J.E., Cross, J.B., Bakken, V., Adamo, C., Jaramillo, J., Gomperts, R., Stratmann, R.E., Yazyev, O., Austin, A.J.,, Cammi, R., Pomelli, C., Ochterski, J.W., Martin, R.L., Morokuma, K., Zakrzewski, V.G., V., G.A., Salvador, P., Dannenberg, J.J., Dapprich, S., Daniels, A.D., Farkas, and O., F., J.B., Ortiz, J.V., Cioslowski, J., Fox, D.J.: Gaussian 09, Revision A.1. Gaussian
- Gibb, S. W., Mantoura, R. F. C. and Liss, P. S.: Ocean-atmosphere exchange and atmospheric speciation of ammonia and methylamines in the region of the NW Arabian Sea, Global Biogeochemical Cycles, 13, 161-177, http://doi.org/10.1029/98gb00743, 1999.

Inc, Wallingford CT., Gaussian 09, Revision A.1. Gaussian Inc, Wallingford CT., 2009.

- Gong, J., Zhu, T., Kipen, H., Wang, G., Hu, M., Guo, Q., Ohman-Strickland, P., Lu, S. E., Wang, Y., Zhu, P., Rich, D. Q., Huang, W. and Zhang, J.: Comparisons of ultrafine and fine particles in their associations with biomarkers reflecting physiological pathways, Environmental Science and Technology, 48, 5264-5273, <a href="http://doi.org/10.1021/es5006016">http://doi.org/10.1021/es5006016</a>, 2014.
  - Gronberg, L., Lovkvist, P. and Jonsson, J. A.: Measurement of aliphatic amines in ambient air and rainwater, Chemosphere, 24, 1533-1540, http://doi.org/10.1016/0045-6535(92)90273-t, 1992.
- Haywood, J. and Boucher, O.: Estimates of the direct and indirect radiative forcing due to tropospheric aerosols: A review,
  Reviews of Geophysics, 38, 513-543, <a href="http://doi.org/Doi.or
- He, X.-C., Simon, M., Iyer, S., Xie, H.-B., Rörup, B., Shen, J., Finkenzeller, H., Stolzenburg, D., Zhang, R., Baccarini, A., Tham, Y. J., Wang, M., Amanatidis, S., Piedehierro, A. A., Amorim, A., Baalbaki, R., Brasseur, Z., Caudillo, L., Chu, B., Dada, L., Duplissy, J., El Haddad, I., Flagan, R. C., Granzin, M., Hansel, A., Heinritzi, M., Hofbauer, V., Jokinen, T., Kemppainen, D., Kong, W., Krechmer, J., Kürten, A., Lamkaddam, H., Lopez, B., Ma, F., Mahfouz, N.
  G. A., Makhmutov, V., Manninen, H. E., Marie, G., Marten, R., Massabò, D., Mauldin, R. L., Mentler, B., Onnela, A., Petäjä, T., Pfeifer, J., Philippov, M., Ranjithkumar, A., Rissanen, M. P., Schobesberger, S., Scholz, W., Schulze, B., Surdu, M., Thakur, R. C., Tomé, A., Wagner, A. C., Wang, D., Wang, Y., Weber, S. K., Welti, A., Winkler, P. M., Zauner-Wieczorek, M., Baltensperger, U., Curtius, J., Kurtén, T., Worsnop, D. R., Volkamer, R., Lehtipalo, K., Kirkby, J., Donahue, N. M., Sipilä, M. and Kulmala, M.: Iodine oxoacids enhance nucleation of sulfuric acid particles in the atmosphere, 382, 1308-1314, http://doi.org/doi:10.1126/science.adh2526, 2023.

- He, X. C., Tham, Y. J., Dada, L., Wang, M. Y., Finkenzeller, H., Stolzenburg, D., Iyer, S., Simon, M., Kurten, A., Shen, J. L., Rorup, B., Rissanen, M., Schobesberger, S., Baalbaki, R., Wang, D. S., Koenig, T. K., Jokinen, T., Sarnela, N., Beck, L. J., Almeida, J., Amanatidis, S., Amorim, A., Ataei, F., Baccarini, A., Bertozzi, B., Bianchi, F., Brilke, S., Caudillo, L., Chen, D. X., Chiu, R., Chu, B. W., Dias, A., Ding, A. J., Dommen, J., Duplissy, J., El Haddad, I., Carracedo, L. 490 G., Granzin, M., Hansel, A., Heinritzi, M., Hofbauer, V., Junninen, H., Kangasluoma, J., Kemppainen, D., Kim, C., Kong, W. M., Krechmer, J. E., Kvashin, A., Laitinen, T., Lamkaddam, H., Lee, C. P., Lehtipalo, K., Leiminger, M., Li, Z. J., Makhmutov, V., Manninen, H. E., Marie, G., Marten, R., Mathot, S., Mauldin, R. L., Mentler, B., Mohler, O., Muller, T., Nie, W., Onnela, A., Petaja, T., Pfeifer, J., Philippov, M., Ranjithkumar, A., Saiz-Lopez, A., Salma, I., Scholz, W., Schuchmann, S., Schulze, B., Steiner, G., Stozhkov, Y., Tauber, C., Tome, A., Thakur, R. C., Vaisanen, 495 O., Vazquez-Pufleau, M., Wagner, A. C., Wang, Y. H., Weber, S. K., Winkler, P. M., Wu, Y. S., Xiao, M., Yan, C., Ye, Q., Ylisirnio, A., Zauner-Wieczorek, M., Zha, Q. Z., Zhou, P. T., Flagan, R. C., Curtius, J., Baltensperger, U., Kulmala, M., Kerminen, V. M., Kurten, T., Donahue, N. M., Volkamer, R., Kirkby, J., Worsnop, D. R. and Sipila, M.: Role of iodine oxoacids atmospheric nucleation, Science, in aerosol 371, 589-+, http://doi.org/10.1126/science.abe0298, 2021.
- Hoffmann, T., O'Dowd, C. D. and Seinfeld, J. H.: Iodine oxide homogeneous nucleation: An explanation for coastal new particle production, Geophysical Research Letters, 28, 1949-1952, <a href="http://doi.org/10.1029/2000gl012399">http://doi.org/10.1029/2000gl012399</a>, 2001.
  - Hu, Q. J., Yu, P. R., Zhu, Y. J., Li, K., Gao, H. W. and Yao, X. H.: Concentration, Size Distribution, and Formation of Trimethylaminium and Dimethylaminium Ions in Atmospheric Particles over Marginal Seas of China\*, Journal of the Atmospheric Sciences, 72, 3487-3498, <a href="http://doi.org/10.1175/jas-d-14-0393.1">http://doi.org/10.1175/jas-d-14-0393.1</a>, 2015.
- Jokinen, T., Sipilä, M., Kontkanen, J., Vakkari, V., Tisler, P., Duplissy, E. M., Junninen, H., Kangasluoma, J., Manninen, H. E., Petäjä, T., Kulmala, M., Worsnop, D. R., Kirkby, J., Virkkula, A. and Kerminen, V. M.: Ion-induced sulfuric acid-ammonia nucleation drives particle formation in coastal Antarctica, Science Advances, 4, <a href="http://doi.org/10.1126/sciadv.aat9744">http://doi.org/10.1126/sciadv.aat9744</a>, 2018.
- Kalivitis, N., Kerminen, V. M., Kouvarakis, G., Stavroulas, I., Bougiatioti, A., Nenes, A., Manninen, H. E., Petäjä, T., Kulmala, M. and Mihalopoulos, N.: Atmospheric new particle formation as a source of CCN in the eastern Mediterranean marine boundary layer, Atmospheric Chemistry and Physics, 15, 9203-9215, <a href="http://doi.org/10.5194/acp-15-9203-2015">http://doi.org/10.5194/acp-15-9203-2015</a>, 2015.
- Kirkby, J., Curtius, J., Almeida, J., Dunne, E., Duplissy, J., Ehrhart, S., Franchin, A., Gagné, S., Ickes, L., Kürten, A., Kupc, A., Metzger, A., Riccobono, F., Rondo, L., Schobesberger, S., Tsagkogeorgas, G., Wimmer, D., Amorim, A., Bianchi, F., Breitenlechner, M., David, A., Dommen, J., Downard, A., Ehn, M., Flagan, R. C., Haider, S., Hansel, A., Hauser, D., Jud, W., Junninen, H., Kreissl, F., Kvashin, A., Laaksonen, A., Lehtipalo, K., Lima, J., Lovejoy, E. R., Makhmutov, V., Mathot, S., Mikkilä, J., Minginette, P., Mogo, S., Nieminen, T., Onnela, A., Pereira, P., Petäjä, T., Schnitzhofer, R., Seinfeld, J. H., Sipilä, M., Stozhkov, Y., Stratmann, F., Tomé, A., Vanhanen, J., Viisanen, Y., Vrtala, A., Wagner, P. E., Walther, H., Weingartner, E., Wex, H., Winkler, P. M., Carslaw, K. S., Worsnop, D. R., Baltensperger, U. and Kulmala, M.: Role of sulphuric acid, ammonia and galactic cosmic rays in atmospheric aerosol nucleation, Nature, 476, 429-U477, http://doi.org/10.1038/nature10343, 2011.
  - Knattrup, Y. and Elm, J.: Clusteromics IV: The Role of Nitric Acid in Atmospheric Cluster Formation, Acs Omega, <a href="http://doi.org/10.1021/acsomega.2c04278">http://doi.org/10.1021/acsomega.2c04278</a>, 2022.
- Kubecka, J., Besel, V., Kurtén, T., Myllys, N. and Vehkamäki, H.: Configurational Sampling of Noncovalent (Atmospheric)

  Molecular Clusters: Sulfuric Acid and Guanidine, Journal of Physical Chemistry A, 123, 6022-6033, 
  http://doi.org/10.1021/acs.jpca.9b03853, 2019.
  - Kurfman, L. A., Odbadrakh, T. T. and Shields, G. C.: Calculating Reliable Gibbs Free Energies for Formation of Gas-Phase Clusters that Are Critical for Atmospheric Chemistry: (H<sub>2</sub>SO<sub>4</sub>)<sub>3</sub>, Journal of Physical Chemistry A, 125, 3169-3176, <a href="http://doi.org/10.1021/acs.jpca.1c00872">http://doi.org/10.1021/acs.jpca.1c00872</a>, 2021.
- Kürten, A., Li, C. X., Bianchi, F., Curtius, J., Dias, A., Donahue, N. M., Duplissy, J., Flagan, R. C., Hakala, J., Jokinen, T., Kirkby, J., Kulmala, M., Laaksonen, A., Lehtipalo, K., Makhmutov, V., Onnela, A., Rissanen, M. P., Simon, M., Sipilä, M., Stozhkov, Y., Tröstl, J., Ye, P. L. and McMurry, P. H.: New particle formation in the sulfuric acid-

- dimethylamine-water system: reevaluation of CLOUD chamber measurements and comparison to an aerosol nucleation and growth model, Atmospheric Chemistry and Physics, 18, 845-863, <a href="http://doi.org/10.5194/acp-18-845-2018">http://doi.org/10.5194/acp-18-845-2018</a>, 2018.
- Kurtén, T., Loukonen, V., Vehkamäki, H. and Kulmala, M.: Amines are likely to enhance neutral and ion-induced sulfuric acid-water nucleation in the atmosphere more effectively than ammonia, Atmospheric Chemistry and Physics, 8, 4095-4103, <a href="http://doi.org/10.5194/acp-8-4095-2008">http://doi.org/10.5194/acp-8-4095-2008</a>, 2008.
- Lee, S.-H., Gordon, H., Yu, H., Lehtipalo, K., Haley, R., Li, Y. and Zhang, R.: New Particle Formation in the Atmosphere:

  From Molecular Clusters to Global Climate, Journal of Geophysical Research: Atmospheres, 124, 7098-7146, 
  http://doi.org/10.1029/2018jd029356, 2019.

550

570

- Liu, L., Li, H., Zhang, H. J., Zhong, J., Bai, Y., Ge, M. F., Li, Z. S., Chen, Y. and Zhang, X. H.: The role of nitric acid in atmospheric new particle formation, Physical Chemistry Chemical Physics, 20, 17406-17414, <a href="http://doi.org/10.1039/c8cp02719f">http://doi.org/10.1039/c8cp02719f</a>, 2018.
- Liu, L., Li, S., Zu, H. and Zhang, X.: Unexpectedly significant stabilizing mechanism of iodous acid on iodic acid nucleation under different atmospheric conditions, Science of The Total Environment, 859, 159832, <a href="http://doi.org/https://doi.org/10.1016/j.scitotenv.2022.159832">http://doi.org/https://doi.org/10.1016/j.scitotenv.2022.159832</a>, 2023.
  - Liu, L., Yu, F. Q., Du, L., Yang, Z., Francisco, J. S. and Zhang, X. H.: Rapid sulfuric acid-dimethylamine nucleation enhanced by nitric acid in polluted regions, Proceedings of the National Academy of Sciences of the United States of America, 118, http://doi.org/10.1073/pnas.2108384118/10f6, 2021a.
  - Liu, L., Yu, F. Q., Tu, K. P., Yang, Z. and Zhang, X. H.: Influence of atmospheric conditions on the role of trifluoroacetic acid in atmospheric sulfuric acid-dimethylamine nucleation, Atmospheric Chemistry and Physics, 21, 6221-6230, <a href="http://doi.org/10.5194/acp-21-6221-2021">http://doi.org/10.5194/acp-21-6221-2021</a>, 2021b.
- Liu, Z. Y., Li, M., Wang, X. F., Liang, Y. H., Jiang, Y. R., Chen, J., Mu, J. S., Zhu, Y. J., Meng, H., Yang, L. X., Hou, K. Y.,

  Wang, Y. F. and Xue, L. K.: Large contributions of anthropogenic sources to amines in fine particles at a coastal area in northern China in winter, Science of the Total Environment, 839, 

  <a href="http://doi.org/10.1016/j.scitotenv.2022.156281">http://doi.org/10.1016/j.scitotenv.2022.156281</a>, 2022.
  - Lu, T. and Chen, F.: Multiwfn: a multifunctional wavefunction analyzer, Journal of computational chemistry, 33, 580-592, 2012a.
- ---. Quantitative analysis of molecular surface based on improved Marching Tetrahedra algorithm, Journal of Molecular Graphics & Modelling, 38, 314-323, <a href="http://doi.org/10.1016/j.jmgm.2012.07.004">http://doi.org/10.1016/j.jmgm.2012.07.004</a>, 2012b.
  - Lu, Y. Q., Liu, L., Ning, A., Yang, G., Liu, Y. L., Kurten, T., Vehkamaki, H., Zhang, X. H. and Wang, L.: Atmospheric Sulfuric Acid-Dimethylamine Nucleation Enhanced by Trifluoroacetic Acid, Geophysical Research Letters, 47, <a href="http://doi.org/10.1029/2019gl085627">http://doi.org/10.1029/2019gl085627</a>, 2020.
- Ma, F. F., Xie, H. B., Zhang, R. J., Su, L. H., Jiang, Q., Tang, W. H., Chen, J. W., Engsvang, M., Elm, J. and He, X. C.: Enhancement of Atmospheric Nucleation Precursors on Iodic Acid- Induced Nucleation: Predictive Model and Mechanism, Environmental Science & Technology, 57, 6944-6954, <a href="http://doi.org/10.1021/acs.est.3c01034">http://doi.org/10.1021/acs.est.3c01034</a>, 2023.
  - Mahajan, A. S., Sorribas, M., Martin, J. C. G., MacDonald, S. M., Gil, M., Plane, J. M. C. and Saiz-Lopez, A.: Concurrent observations of atomic iodine, molecular iodine and ultrafine particles in a coastal environment, Atmospheric Chemistry and Physics, 11, 2545-2555, <a href="http://doi.org/10.5194/acp-11-2545-2011">http://doi.org/10.5194/acp-11-2545-2011</a>, 2011.
  - McFiggans, G., Bale, C. S. E., Ball, S. M., Beames, J. M., Bloss, W. J., Carpenter, L. J., Dorsey, J., Dunk, R., Flynn, M. J., Furneaux, K. L., Gallagher, M. W., Heard, D. E., Hollingsworth, A. M., Hornsby, K., Ingham, T., Jones, C. E., Jones, R. L., Kramer, L. J., Langridge, J. M., Leblanc, C., LeCrane, J. P., Lee, J. D., Leigh, R. J., Longley, I., Mahajan, A. S., Monks, P. S., Oetjen, H., Orr-Ewing, A. J., Plane, J. M. C., Potin, P., Shillings, A. J. L., Thomas, F., von Glasow, R., Wada, R., Whalley, L. K. and Whitehead, J. D.: Iodine-mediated coastal particle formation: an overview of the Reactive Halogens in the Marine Boundary Layer (RHaMBLe) Roscoff coastal study, Atmospheric Chemistry and Physics, 10, 2975-2999, http://doi.org/10.5194/acp-10-2975-2010, 2010.
  - McGrath, M. J., Olenius, T., Ortega, I. K., Loukonen, V., Paasonen, P., Kurtén, T., Kulmala, M. and Vehkamäki, H.: Atmospheric Cluster Dynamics Code: a flexible method for solution of the birth-death equations, Atmospheric

590

605

- Müller, C., Iinuma, Y., Karstensen, J., van Pinxteren, D., Lehmann, S., Gnauk, T. and Herrmann, H.: Seasonal variation of aliphatic amines in marine sub-micrometer particles at the Cape Verde islands, Atmospheric Chemistry and Physics, 9, 9587-9597, 2009.
- Murphy, D. M. and Ravishankara, A. R.: Trends and patterns in the contributions to cumulative radiative forcing from different regions of the world, Proceedings of the National Academy of Sciences of the United States of America, 115, 13192-13197, http://doi.org/10.1073/pnas.1813951115, 2018.
  - Nault, B. A., Campuzano-Jost, P., Day, D. A., Jo, D. S., Schroder, J. C., Allen, H. M., Bahreini, R., Bian, H. S., Blake, D. R., Chin, M., Clegg, S. L., Colarco, P. R., Crounse, J. D., Cubison, M. J., DeCarlo, P. F., Dibb, J. E., Diskin, G. S., Hodzic, A., Hu, W. W., Katich, J. M., Kim, M. J., Kodros, J. K., Kupc, A., Lopez-Hilfiker, F. D., Marais, E. A., Middlebrook, A. M., Neuman, J. A., Nowak, J. B., Palm, B. B., Paulot, F., Pierce, J. R., Schill, G. P., Scheuer, E., Thornton, J. A., Tsigaridis, K., Wennberg, P. O., Williamson, C. J. and Jimenez, J. L.: Chemical transport models often underestimate inorganic aerosol acidity in remote regions of the atmosphere, Communications Earth & Environment, 2, http://doi.org/10.1038/s43247-021-00164-0, 2021.
- Ning, A., Liu, L., Zhang, S. B., Yu, F. Q., Du, L., Ge, M. F. and Zhang, X. H.: The critical role of dimethylamine in the rapid formation of iodic acid particles in marine areas, NPJ Climate and Atmospheric Science, 5, http://doi.org/10.1038/s41612-022-00316-9, 2022.
  - O'Dowd, C. D. and de Leeuw, G.: Marine aerosol production: a review of the current knowledge, Philos Trans A Math Phys Eng Sci, 365, 1753-1774, http://doi.org/10.1098/rsta.2007.2043, 2007.
- O'Dowd, C. D., Hämeri, K., Mäkelä, J., Väkeva, M., Aalto, P., de Leeuw, G., Kunz, G. J., Becker, E., Hansson, H. C., Allen,
  A. G., Harrison, R. M., Berresheim, H., Geever, M., Jennings, S. G. and Kulmala, M.: Coastal new particle
  formation:: Environmental conditions and aerosol physicochemical characteristics during nucleation bursts -: art. no.
  8107, Journal of Geophysical Research-Atmospheres, 107, <a href="http://doi.org/10.1029/2000jd000206">http://doi.org/10.1029/2000jd000206</a>, 2002a.
  - O'Dowd, C. D., Hämeri, K., Mäkelä, J. M., Pirjola, L., Kulmala, M., Jennings, S. G., Berresheim, H., Hansson, H.-C., de Leeuw, G., Kunz, G. J., Allen, A. G., Hewitt, C. N., Jackson, A., Viisanen, Y. and Hoffmann, T.: A dedicated study of new particle formation and fate in the coastal environment: overview of objectives and achievements, Journal of Geophysical Research: Atmospheres, 107, 1-16, <a href="http://doi.org/10.1029/2001jd000555">http://doi.org/10.1029/2001jd000555</a>, 2002b.
  - O'Dowd, C. D., Jimenez, J. L., Bahreini, R., Flagan, R. C., Seinfeld, J. H., Hämeri, K., Pirjola, L., Kulmala, M., Jennings, S. G. and Hoffmann, T.: Marine aerosol formation from biogenic iodine emissions, Nature, 417, 632-636, <a href="http://doi.org/10.1038/nature00775">http://doi.org/10.1038/nature00775</a>, 2002c.
- Olenius, T., Halonen, R., Kurtén, T., Henschel, H., Kupiainen-Määtä, O., Ortega, I. K., Jen, C. N., Vehkamäki, H. and Riipinen, I.: New particle formation from sulfuric acid and amines: Comparison of monomethylamine, dimethylamine, and trimethylamine, Journal of Geophysical Research-Atmospheres, 122, 7103-7118, <a href="http://doi.org/10.1002/2017jd026501">http://doi.org/10.1002/2017jd026501</a>, 2017.
- Peterson, K. A.: Systematically convergent basis sets with relativistic pseudopotentials. I. Correlation consistent basis sets for the post-d group 13–15 elements, The Journal of Chemical Physics, 119, 11099-11112, http://doi.org/10.1063/1.1622923, 2003.
  - Pope, C. A., III and Dockery, D. W.: Health effects of fine particulate air pollution: lines that connect, Journal of the Air & Waste Management Association, 56, 709-742, <a href="http://doi.org/10.1080/10473289.2006.10464485">http://doi.org/10.1080/10473289.2006.10464485</a>, 2006.
- Quéléver, L. L. J., Dada, L., Asmi, E., Lampilahti, J., Chan, T., Ferrara, J. E., Copes, G. E., Pérez-Fogwill, G., Barreira, L., Aurela, M., Worsnop, D. R., Jokinen, T. and Sipilä, M.: Investigation of new particle formation mechanisms and aerosol processes at Marambio Station, Antarctic Peninsula, Atmospheric Chemistry and Physics, 22, 8417-8437, <a href="http://doi.org/10.5194/acp-22-8417-2022">http://doi.org/10.5194/acp-22-8417-2022</a>, 2022.
  - Rappé, A. K., Casewit, C. J., Colwell, K. S., Goddard, W. A. and Skiff, W. M.: UFF, a Full Periodic-Table Force-Field for Molecular Mechanics and Molecular-Dynamics Simulations, Journal of the American Chemical Society, 114, 10024-10035, 1992.
  - Rong, H., Liu, J., Zhang, Y., Du, L., Zhang, X. and Li, Z.: Nucleation mechanisms of iodic acid in clean and polluted coastal

- regions, Chemosphere, 253, 126743, http://doi.org/10.1016/j.chemosphere.2020.126743, 2020.
- Schmitz, G.: Inorganic reactions of iodine(III) in acidic solutions and free energy of iodous acid formation, International Journal of Chemical Kinetics, 40, 647-652, http://doi.org/10.1002/kin.20344, 2008.
- Shampine, L. and Reichelt, M.: The MATLAB ODE suite. SIAM J. Sci. Comput. 18 (1), 1–22, Siam Journal on Scientific Computing, 18, 1-22, 1997.
  - Shen, J. W., Elm, J., Xie, H. B., Chen, J. W., Niu, J. F. and Vehkamäki, H.: Structural Effects of Amines in Enhancing Methanesulfonic Acid-Driven New Particle Formation, Environmental Science & Technology, 54, 13498-13508, http://doi.org/10.1021/acs.est.0c05358, 2020.
- Sipilä, M., Sarnela, N., Jokinen, T., Henschel, H., Junninen, H., Kontkanen, J., Richters, S., Kangasluoma, J., Franchin, A., Peräkylä, O., Rissanen, M. P., Ehn, M., Vehkamäki, H., Kurten, T., Berndt, T., Petäjä, T., Worsnop, D., Ceburnis, D., Kerminen, V. M., Kulmala, M. and O'Dowd, C.: Molecular-scale evidence of aerosol particle formation via sequential addition of HIO<sub>3</br>

- Stewart, J. J.: Stewart Computational Chemistry, Colorado Springs, CO, USA, MOPAC 2016, Stewart Computational Chemistry, Colorado Springs, CO, USA, 2016.
- Stewart, J. J. P.: Optimization of parameters for semiempirical methods VI: more modifications to the NDDO approximations and re-optimization of parameters, Journal of Molecular Modeling, 19, 1-32, http://doi.org/10.1007/s00894-012-1667-x, 2013.
- Vanneste, A., Duce, R. A. and Lee, C.: Methylamines in the marine atmosphere, Geophysical Research Letters, 14, 711-714, http://doi.org/10.1029/GL014i007p00711, 1987.
- Wang, J. Y., Xu, G. J., Chen, L. Q. and Chen, K.: Atmospheric Particle Number Concentrations and New Particle Formation over the Southern Ocean and Antarctica: A Critical Review, Atmosphere, 14, <a href="http://doi.org/10.3390/atmos14020402">http://doi.org/10.3390/atmos14020402</a>, 2023.
- Wang, M. Y., Kong, W. M., Marten, R., He, X. C., Chen, D. X., Pfeifer, J., Heitto, A., Kontkanen, J., Dada, L., Kurten, A.,
  Yli-Juuti, T., Manninen, H. E., Amanatidis, S., Amorim, A., Baalbaki, R., Baccarini, A., Bell, D. M., Bertozzi, B.,
  Bräkling, S., Brilke, S., Murillo, L. C., Chiu, R., Chu, B. W., De Menezes, L. P., Duplissy, J., Finkenzeller, H.,
  Carracedo, L. G., Granzin, M., Guida, R., Hansel, A., Hofbauer, V., Krechmer, J., Lehtipalo, K., Lamkaddam, H.,
  Lampimäki, M., Lee, C. P., Makhmutov, V., Marie, G., Mathot, S., Mauldin, R. L., Mentler, B., Muller, T., Onnela,
  A., Partoll, E., Petäjä, T., Philippov, M., Pospisilova, V., Ranjithkumar, A., Rissanen, M., Rörup, B., Scholz, W.,
  Shen, J. L., Simon, M., Sipilä, M., Steiner, G., Stolzenburg, D., Tham, Y. J., Tomé, A., Wagner, A. C., Wang, D. Y.
  S., Wang, Y. H., Weber, S. K., Winkler, P. M., Wlasits, P. J., Wu, Y. H., Xiao, M., Ye, Q., Zauner-Wieczorek, M.,
  Zhou, X. Q., Volkamer, R., Riipinen, I., Dommen, J., Curtius, J., Baltensperger, U., Kulmala, M., Worsnop, D. R.,
  Kirkby, J., Seinfeld, J. H., El-Haddad, I., Flagan, R. C. and Donahue, N. M.: Rapid growth of new atmospheric particles by nitric acid and ammonia condensation, Nature, 581, 184-+, <a href="http://doi.org/10.1038/s41586-020-2270-4">http://doi.org/10.1038/s41586-020-2270-4</a>,
  2020.
- Wang, M. Y., Xiao, M., Bertozzi, B., Marie, G., Rörup, B., Schulze, B., Bardakov, R., He, X. C., Shen, J. L., Scholz, W., Marten, R., Dada, L., Baalbaki, R., Lopez, B., Lamkaddam, H., Manninen, H. E., Amorim, A., Ataei, F., Bogert, P., Brasseur, Z., Caudillo, L., De Menezes, L. P., Duplissy, J., Ekman, A. M. L., Finkenzeller, H., Carracedo, L. G., Granzin, M., Guida, R., Heinritzi, M., Hofbauer, V., Höhler, K., Korhonen, K., Krechmer, J. E., Kürten, A., Lehtipalo, K., Mahfouz, N. G. A., Makhmutov, V., Massabò, D., Mathot, S., Mauldin, R. L., Mentler, B., Müller, T., Onnela, A., Petäjä, T., Philippov, M., Piedehierro, A. A., Pozzer, A., Ranjithkumar, A., Schervish, M., Schobesberger, S., Simon, M., Stozhkov, Y., Tomé, A., Umo, N. S., Vogel, F., Wagner, R., Wang, D. S., Weber, S. K., Welti, A., Wu, Y. S., Zauner-Wieczorek, M., Sipilä, M., Winkler, P. M., Hansel, A., Baltensperger, U., Kulmala, M., Flagan, R. C., Curtius, J., Riipinen, I., Gordon, H., Lelieveld, J., El-Haddad, I., Volkamer, R., Worsnop, D. R., Christoudias, T., Kirkby, J., Möhler, O. and Donahue, N. M.: Synergistic HNO<sub>3</sub>-H<sub>2</sub>SO<sub>4</sub>-NH<sub>3</sub> upper tropospheric particle formation, Nature, 605, 483-+, <a href="http://doi.org/10.1038/s41586-022-04605-4">http://doi.org/10.1038/s41586-022-04605-4</a>, 2022.
  - Weber, R. J., Marti, J. J., McMurry, P. H., Eisele, F. L., Tanner, D. J. and Jefferson, A.: Measured atmospheric new particle

- formation rates: Implications for nucleation mechanisms, Chemical Engineering Communications, 151, 53-64, <a href="http://doi.org/10.1080/00986449608936541">http://doi.org/10.1080/00986449608936541</a>, 1996.
  - Xia, D., Chen, J., Yu, H., Xie, H. B., Wang, Y., Wang, Z., Xu, T. and Allen, D. T.: Formation Mechanisms of Iodine-Ammonia Clusters in Polluted Coastal Areas Unveiled by Thermodynamic and Kinetics Simulations, Environmental Science & Technology, 54, 9235-9242, http://doi.org/10.1021/acs.est.9b07476, 2020.
- Xie, H. B. and Elm, J.: Tri-Base Synergy in Sulfuric Acid-Base Clusters, Atmosphere, 12, http://doi.org/10.3390/atmos12101260, 2021.
  - Yang, Y., Waller, S. E., Kreinbihl, J. J. and Johnson, C. J.: Direct Link between Structure and Hydration in Ammonium and Aminium Bisulfate Clusters Implicated in Atmospheric New Particle Formation, Journal of Physical Chemistry Letters, 9, 5647-5652, http://doi.org/10.1021/acs.jpclett.8b02500, 2018.
- Yang, Y., Weaver, M. N. and Merz, K. M.: Assessment of the "6-31+G\*\*+LANL2DZ" Mixed Basis Set Coupled with Density Functional Theory Methods and the Effective Core Potential: Prediction of Heats of Formation and Ionization Potentials for First-Row-Transition-Metal Complexes, Journal of Physical Chemistry A, 113, 9843-9851, http://doi.org/10.1021/jp807643p, 2009.
  - Yao, L., Garmash, O., Bianchi, F., Zheng, J., Yan, C., Kontkanen, J., Junninen, H., Mazon, S. B., Ehn, M., Paasonen, P., Sipila, M., Wang, M. Y., Wang, X. K., Xiao, S., Chen, H. F., Lu, Y. Q., Zhang, B. W., Wang, D. F., Fu, Q. Y., Geng, F. H., Li, L., Wang, H. L., Qiao, L. P., Yang, X., Chen, J. M., Kerminen, V. M., Petaja, T., Worsnop, D. R., Kulmala, M. and Wang, L.: Atmospheric new particle formation from sulfuric acid and amines in a Chinese megacity, Science, 361, 278-281, http://doi.org/10.1126/science.aao4839, 2018.
  - Yu, F. and Luo, G.: Modeling of gaseous methylamines in the global atmosphere: impacts of oxidation and aerosol uptake, Atmospheric Chemistry and Physics, 14, 12455-12464, http://doi.org/10.5194/acp-14-12455-2014, 2014.
- Yu, H., Ren, L., Huang, X., Xie, M., He, J. and Xiao, H.: Iodine speciation and size distribution in ambient aerosols at a coastal new particle formation hotspot in China, Atmospheric Chemistry and Physics, 19, 4025-4039, http://doi.org/10.5194/acp-19-4025-2019, 2019.
  - Zhang, J. and Dolg, M.: ABCluster: the artificial bee colony algorithm for cluster global optimization, Physical Chemistry Chemical Physics, 17, 24173-24181, 2015.
- Zhang, M. M., Yan, J. P., Lin, Q., Park, K., Zhao, S. H., Xu, S. Q. and Wang, S. S.: Low contributions of dimethyl sulfide (DMS) chemistry to atmospheric aerosols over the high Arctic Ocean, Atmospheric Environment, 313, <a href="http://doi.org/10.1016/j.atmosenv.2023.120073">http://doi.org/10.1016/j.atmosenv.2023.120073</a>, 2023.
  - Zhang, R.: Getting to the Critical Nucleus of Aerosol Formation, Science, 328, 1366-1367, 2010.

- Zhang, R., Khalizov, A., Wang, L., Hu, M. and Xu, W.: Nucleation and growth of nanoparticles in the atmosphere, Chemical Reviews, 112, 1957-2011, <a href="http://doi.org/10.1021/cr2001756">http://doi.org/10.1021/cr2001756</a>, 2012.
- Zhang, R. J., Xie, H. B., Ma, F. F., Chen, J. W., Iyer, S., Simon, M., Heinritzi, M., Shen, J. L., Tham, Y. J., Kurten, T., Worsnop, D. R., Kirkby, J., Curtius, J., Sipila, M., Kulmala, M. and He, X. C.: Critical Role of Iodous Acid in Neutral Iodine Oxoacid Nucleation, Environmental Science & Technology, <a href="http://doi.org/10.1021/acs.est.2c04328">http://doi.org/10.1021/acs.est.2c04328</a>, 2022a.
- Zhang, S. B., Li, S. N., Ning, A., Liu, L. and Zhang, X. H.: Iodous acid a more efficient nucleation precursor than iodic acid, Physical Chemistry Chemical Physics, 24, 13651-13660, <a href="http://doi.org/10.1039/d2cp00302c">http://doi.org/10.1039/d2cp00302c</a>, 2022b.
  - Zhu, Y. J., Li, K., Shen, Y. J., Gao, Y., Liu, X. H., Yu, Y., Gao, H. W. and Yao, X. H.: New particle formation in the marine atmosphere during seven cruise campaigns, Atmospheric Chemistry and Physics, 19, 89-113, <a href="http://doi.org/10.5194/acp-19-89-2019">http://doi.org/10.5194/acp-19-89-2019</a>, 2019.
- Zu, H. T., Zhang, S. B., Liu, L. and Zhang, X. H.: The vital role of sulfuric acid in iodine oxoacids nucleation: impacts of urban pollutants on marine atmosphere, Environmental Research Letters, 19, <a href="http://doi.org/10.1088/1748-9326/ad193f">http://doi.org/10.1088/1748-9326/ad193f</a>, 2024.